RepGhost: A Hardware-Efficient Ghost Module via Re-parameterization

Chengpeng Chen[*], **Zichao Guo**[*†], **Haien Zeng**, **Pengfei Xiong**, **Jian Dong**
Shopee

Abstract

Feature reuse has been a key technique in light-weight convolutional neural networks (CNNs) architecture design. Current methods usually utilize a concatenation operator to keep large channel numbers cheaply (thus large network capacity) by reusing feature maps from other layers. Although concatenation is parameters- and FLOPs-free, its computational cost on hardware devices is non-negligible. To address this, this paper provides a new perspective to realize feature reuse implicitly and more efficiently instead of concatenation. A novel hardware-efficient RepGhost module is proposed for implicit feature reuse via re-parameterization, instead of using concatenation operator. Based on the RepGhost module, we develop our efficient RepGhost bottleneck and RepGhostNet. Experiments on ImageNet and COCO benchmarks demonstrate that our RepGhostNet is much more effective and efficient than GhostNet and MobileNetV3 on mobile devices. Specially, our RepGhostNet surpasses GhostNet $0.5\times$ by 2.5% Top-1 accuracy on ImageNet dataset with less parameters and comparable latency on an ARM-based mobile device. Code and model weights are available at `https://github.com/ChengpengChen/RepGhost`.

1 Introduction

With the mobile and portable devices being ubiquitous, efficient convolutional neural networks (CNNs) are becoming indispensable due to the limited computational resources. Different methods are proposed to achieve the same goal of making CNNs more efficient in recent years, such as light-weight architecture design [32, 19, 38, 50, 3], neural architecture search [41, 27, 12, 48], pruning [30, 33, 2, 17], etc, and a lot of progress has been made.

In the field of CNNs architecture design, large channel numbers often means large network capacity [16, 23], especially for light-weight CNNs [32, 18]. As stated in [32], given a fixed floating-point operations (FLOPs), the light-weight CNNs prefer to use *spare connections* (*e.g.*, group or depth-wise convolution) and *feature reuse*. They both have been well-explored and many representative light-weight CNNs have been proposed in recent years [19, 18, 49, 32, 50, 5]. Spare connections are designed to keep large network capacity with low FLOPs, while feature reuse aims to *explicitly* keep large number of channel by simply preserving existing features from different layers, which is often achieved by concatenation operations along channel dimension [23, 13, 40]. For example, in DenseNet, feature maps from previous layers are reused and sent to their subsequent layers within a stage, resulting in more and more channels. GhostNet proposes to generate more feature maps from cheap operations, and concatenate them with original ones for keeping large number of channels. ShuffleNetV2 processes only half of channels and keeps the other half to be concatenated. They all utilize the feature reuse approach via concatenation to enlarge channel numbers while keeping

---

[*]Joint first authors.
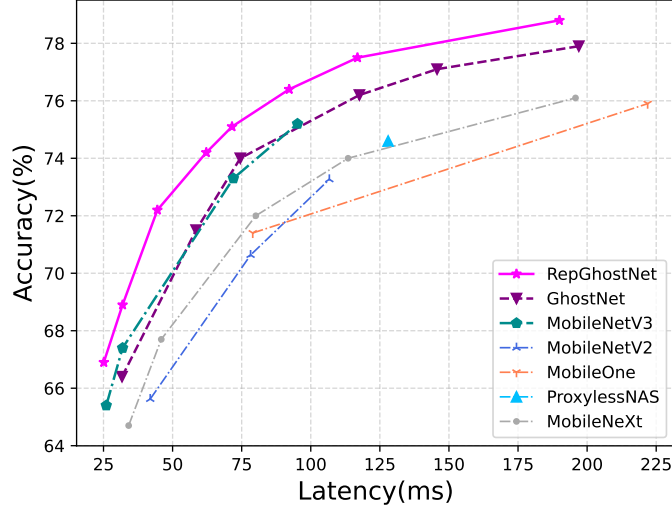
[†]Corresponding author.

Figure 1: Top-1 accuracy on ImageNet dataset **vs.** latency on an ARM-based mobile device, refer to Section 4 for the detail and Appendix A for more running devices.

FLOPs low. It seems that concatenation has been a standard and elegant operation for feature reuse, since it is parameters- and FLOPs-free.

However, parameters and FLOPs are not direct cost indicators for actual runtime performance of machine learning models [7, 32]. Although concatenation operation is parameters- and FLOPs-free, its computational cost on hardware devices is non-negligible. To verify this, we provide detailed analysis in Section 3.1 and find that concatenation operation is much more inefficient than add operation on hardware devices due to its complicated memory copy process. Therefore, it is noteworthy to explore a better and more hardware-efficient way for feature reuse beyond concatenation operation.

Recently, structural re-parameterization has proved its effectiveness in CNNs architecture design, including ExpandNets [11], ACNet [9], and RepVGG [10]. It converts complex training-time architectures into simpler inference-time ones equivalently without any extra inference costs. Inspired by this, we propose to utilize structural re-parameterization, instead of the widely-used concatenation, to realize feature reuse *implicitly* for hardware-efficient architecture design.

In this paper, we propose a hardware-efficient RepGhost module via structural re-parameterization to realize feature reuse implicitly. Note that it is not just to apply re-parameterization technique to Ghost module, but to design our novel and efficient module for fast inference. To be specific, we first remove the inefficient concatenation operator, and then modify the architecture to satisfy the rule of structural re-parameterization. Therefore, the feature reuse process can be moved from feature space to weight space during inference, $i.e.$, to reuse features implicitly and efficiently. Based on RepGhost module, our hardware-efficient CNN *RepGhostNet* outperforms state-of-the-art (SOTA) light-weight CNNs in accuracy-latency trade-off, as shown in Figure 1. Our contributions are summarized as:

- We show that concatenation operation is not cost-free and indispensable for feature reuse in hardware-efficient architecture design, and propose a new perspective to realize feature reuse via structural re-parameterization technique.

- We are the first to utilize re-parameterization for simplifying network topology and improving hardware-efficiency, instead of its regular usage to boost performance [9, 10], which does not change the network.

- We propose a novel RepGhost module with implicit feature reuse and develop a more hardware-efficient RepGhostNet compared to SOTA light-weight CNNs [18, 13, 32]. We show that RepGhostNet can achieve better accuracy-latency trade-off on several vision tasks.

2 Related Work

2.1 Light-weight CNNs

Both manual designed [19, 49, 38] and neural architecture search (NAS) [48, 46, 12, 21] based light-weight CNNs are mainly designed to get competitive performances with less parameters and low FLOPs. Among them, ShuffleNetV1 [49] and MobileNetV2 [38] establish the benchmark by using massive depthwise convolutions rather than the dense ones. FBNet [48, 46] employ complex NAS technique to design light-weight architecture automatically. However, parameters and FLOPs often can not reflect the actual runtime performance (*i.e.*, latency) of light-weight CNNs [32, 7]. Only few models are designed for low latency directly, like ProxylessNAS [27], MNASNet [41], MobileNetV3 [18], and ShuffleNetV2 [32]. This paper follows this idea to design low-latency and efficient CNNs.

On the other hand, feature reuse in CNNs has also inspired many impressive works [23, 22, 13, 14, 32, 40] with cheap or even free costs. As light-weight CNNs, GhostNet [13] uses cheap operations to produce more channels with low computational costs, and ShuffleNetV2 [32] processes only half of channels of features and keep the other half to be concatenated. They all use concatenation operation to keep large channel numbers since it is parameters- and FLOPs-free. But we note that it is inefficient on mobile devices due to its complicated memory copy process, making it not indispensable for feature reuse in light-weight CNNs. Therefore, in this paper, we explore to utilize feature reuse in light-weight CNNs architecture design beyond concatenation operation.

2.2 Structural Re-parameterization

Structural re-parameterization is generally to transform the more expressive and complex architecture at training time into a simpler one during inference, thus improving performance without any extra inference cost. ExpandNets [11] expands the linear layers in the model into several continuous linear layers during training. ACNet [9] and RepVGG [10] decompose a single convolutional layer into a training-time multi-branch block. For example, one such training-time block in RepVGG contains three parallel layers, *i.e.*, 3×3 convolution, 1×1 convolution and identity mapping, and an add operator to fuse their output features. During inference, the fusion process can be moved from feature space to weight space, resulting in a simpler block for fast inference (only one 3×3 convolution) [10]. Recently, this technique is also employed by MobileOne [45] to improve performance and design mobile backbones with large FLOPs for the powerful NPU in iPhone12.

All of these works build / have their CNNs firstly, and then utilize structural re-parameterization technique to improve the performance, *e.g.*, for existing CNNs [9, 11] and specially designed CNNs with only 3×3 convolution [10] or without shortcuts [45]. However, instead of merely utilizing re-parameterization for performance gain, this paper explores to use this technique to reuse features implicitly and simplify network topology for fast inference.

3 Method

In this section, we will first revisit concatenation operation for feature reuse, and introduce how to utilize structural re-parameterization to achieve this. Based on it, we propose a novel re-parameterized module for implicit feature reuse, *i.e.*, RepGhost module. After that, we describe our hardware-efficient network built on this module, which is denoted as RepGhostNet. We also discuss the role of re-parameterization in our method, which is quite different from those of other works.

3.1 Feature Reuse via Re-parameterization

Feature reuse has been widely used in CNNs to enlarge the network capacity, such as DenseNet [23], ShuffleNetV2 [32] and GhostNet [13]. Most methods utilize the concatenation operator combining feature maps from different layers to produce more features cheaply. Concatenation is parameters- and FLOPs-free, however, its computational cost is non-negligible due to the complicated memory copy on hardware devices. To address this, we provide a new perspective to realize feature reuse implicitly: *feature reuse via structural re-parameterization*.

Concatenation costs. As mentioned above, memory copy in concatenation brings non-negligible computational costs on hardware devices. For example, let $M_1 \in \mathbb{R}^{N \times C_1 \times H \times W}$ and $M_2 \in \mathbb{R}^{N \times C_2 \times H \times W}$ be two feature maps in data layout NCHW[1] to be concatenated alone channel dimension. The largest contiguous blocks of memory required when processing M_1 and M_2 are $b_1 \in \mathbb{R}^{1 \times C_1 \times H \times W}$ and $b_2 \in \mathbb{R}^{1 \times C_2 \times H \times W}$, respectively. Concatenating b_1 and b_2 is direct, and this process would repeat N times [2]. For data in layout NHWC [1], the largest contiguous block of memory is much smaller, i.e., $b_1 \in \mathbb{R}^{1 \times 1 \times 1 \times C_1}$, making the copy process more complicated. While for element-wise operators, like Add, the largest contiguous blocks of memory are M_1 and M_2 themselves, making the operations much easier.

To evaluate the concatenation operation quantitatively, we analyze its actual runtime on an ARM-based mobile device. We take GhostNet 1.0x [13] as an example, and replace all its concatenation operators with add operators for comparison, which is also a simple operator to process different features with low costs [16, 39]. Note that these two operators operate on tensors with exactly the same shape. Table 1 shows the accumulated runtime of all 32 corresponding operators in the corresponding network. Concatenation costs $\sim 2x$ times over Add. We also plot the time percentages under different batch sizes in Figure 2. With batch size increases, the gap of runtime percentage becomes larger, which is consistent with our data layout analysis.

Table 1: Runtime of concatenation and add operators with different batch sizes.

Operator	Latency(ms)			
	bs=1	2	8	32
Concatenation	5.2	13.2	64.2	292.2
Add	2.6	6.7	34.0	149.8

Re-parameterization *vs.* Concatenation Let $y \in \mathbb{R}^{N \times C_{out} \times H \times W}$ denotes the output with C_{out} channels and $x \in \mathbb{R}^{N \times C_{in} \times H \times W}$ the input to be processed and reused. $\Phi_i(x), \forall i = 1, \ldots, s-1$ denote other layers, such as convolution or BN, applied to x. Without loss of generality, feature reuse via concatenation can be expressed as:

$$y = Cat([x, \Phi_1(x), \ldots, \Phi_{s-1}(x)]) \qquad (1)$$

where Cat is the concatenation operation. It simply keeps existing feature maps and leaves the information processing to other operators. For example, a concatenation layer is usually followed by an 1×1 dense convolutional layer to process the channel information [40, 23, 13]. However, as Table 1 shows, concatenation is not cost-free for feature reuse on hardware devices, which motivates us to find a more efficient way.
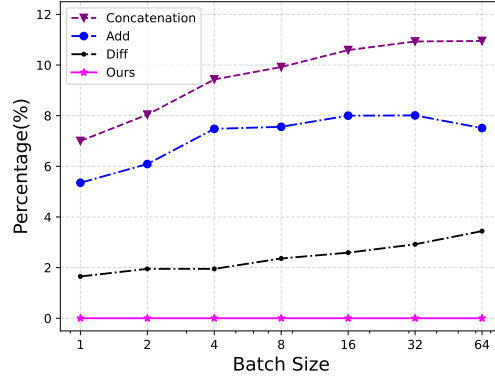

Figure 2: Runtime percentage of each operator in the entire network. **Diff:** the percent difference between concatenation and add. **Ours:** our method takes the add operator as an intermediate state, and it can be fused for fast inference.

Recently, structural re-parameterization has been treated as a cost-free technique to improve the performance of CNNs in many works [9, 10, 45]. Inspired by this, we note that structural re-parameterization can also be treated as an efficient technique for implicit feature reuse, so as to design more hardware-efficient CNNs. For example, structural re-parameterization usually utilizes several linear operators to produce diverse feature maps during training, and fuse all operators into one via parameters fusion for fast inference. That is, it moves the fusion process from feature space to weight space, which can be treated as an implicit way for feature reuse. Follow the symbols in Eq 1, feature reuse via structural re-parameterization can be expressed as:

$$y = Add([x, \Phi_1(x), \ldots, \Phi_{s-1}(x)]) = \Phi^*(x) \qquad (2)$$

Different from concatenation, add also plays a feature fusion role. All operation $\Phi_i(x), \forall i = 1, \ldots, s-1$ in structural re-parameterization are linear function, and will be fused into $\Phi^*(x)$ finally.

---

[1]Data layout NCHW4 is the same case as NCHW.

[2]For batch size 1, pre-allocating memories can omit the copy process, but it needs operator-level optimization.

The feature fusion process is done in the weight space, which will not introduce any extra inference time, making the final architecture more efficient than that with concatenation or add operators.

As shown in Figure 2, our method implements feature reuse via structural re-parameterization. We not only discard the concatenation operator but also move the add process to weight space, thus saving $7\% \sim 11\%$ time compared to concatenation and $5\% \sim 8\%$ to add. Based on this concept, we propose a hardware-efficient module for feature reuse via re-parameterization in the next subsection.

3.2 RepGhost Module

To utilize feature reuse via re-parameterization, this subsection introduces how Ghost module evolves to our RepGhost module. It is non-trivial to apply re-parameterization to original Ghost module directly due to concatenation operator. As Figure 3 shows, we start from Ghost module in Figure 3a and several adjustments are made to derive our RepGhost module.
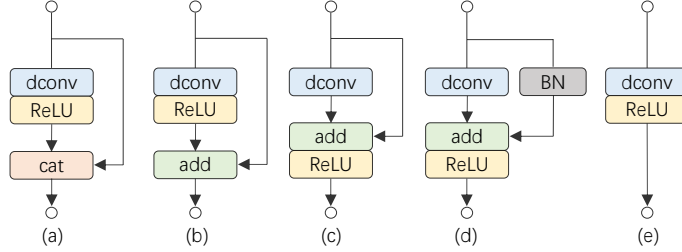

Figure 3: Evolution from Ghost module to RepGhost module. We omit the input 1×1 convolution for simplicity, refer to Figure 4 for more structure details. **dconv:** depthwise convolutional layer. **cat**: concatenation layer. a) Ghost module [13] with ReLU; b) replacing concatenation with add; c) moving ReLU backward to make the module satisfying the rule of structural re-parameterization; d) **RepGhost module** during training; e) RepGhost module during inference.

Add Operator. Due to the inefficiency of concatenation for feature reuse discussed in Section 3.1, we first replace concatenation operator with add operator [16, 39] to get module b in Figure 3. It should provide higher efficiency as shown in Table 1 and Figure 2.

Moving ReLU Backward. In the spirit of structural re-parameterization [9, 10], we move the ReLU after depthwise convolutional layer backward, $i.e.$, after add operator, as module c shown in Figure 3. This movement makes the module satisfying the rule of structural re-parameterization [10, 9], and thus available to be fused into module e for fast inference. We will discuss this in Section 4.3.

Re-parameterization. As a re-parameterized module, module c can be more flexible in the re-parameterization structure rather than identity mapping [9, 45]. As module d shown in Figure 3, we simply add Batch Normalization(BN) [24] in the identity branch, which brings non-linearity during training and can be fused during inference. It is denoted as our **RepGhost module**. We also explore other re-parameterization structures in Section 4.3.

Fast Inference. As re-parameterized modules, module c and module d can be fused into module e in Figure 3 for fast inference. Our RepGhost module has a simple inference structure which only contains a regular convolutional layer and a ReLU, making it hardware-efficient [10]. Specifically, the feature fusion process is carried out in weight space, $i.e.$, fusing parameter of each branch and producing a simplified topology for fast inference. Due to the linearity of each operator, the parameter fusion process is direct (see [9, 10] for the detail).

Comparison with Ghost module. GhostNet [13] proposes to generate more feature maps from cheap operations, thus enlarging the network capacity in a low-cost way. In our RepGhost module, we further propose a more efficient way to generate and fuse diverse feature maps via re-paramterization. Different from Ghost module, RepGhost module removes the inefficient concatenation operator, saving much inference time. And the information fusion process is executed by add operator in an implicit way, instead of leaving to other convolutional layers.

Ghost module [13] has a ratio s to control the complexity. According to Eq 1, $C_{in} = \frac{1}{s} * C_{out}$ and the rest $\frac{s-1}{s} * C_{out}$ channels are produced by depthwise convolutions $\Phi_i, \forall i = 1, \ldots, s - 1$. While for our RepGhost module, $C_{in} = C_{out}$. It produces diverse feature maps with $s * C_{in}$ channels during
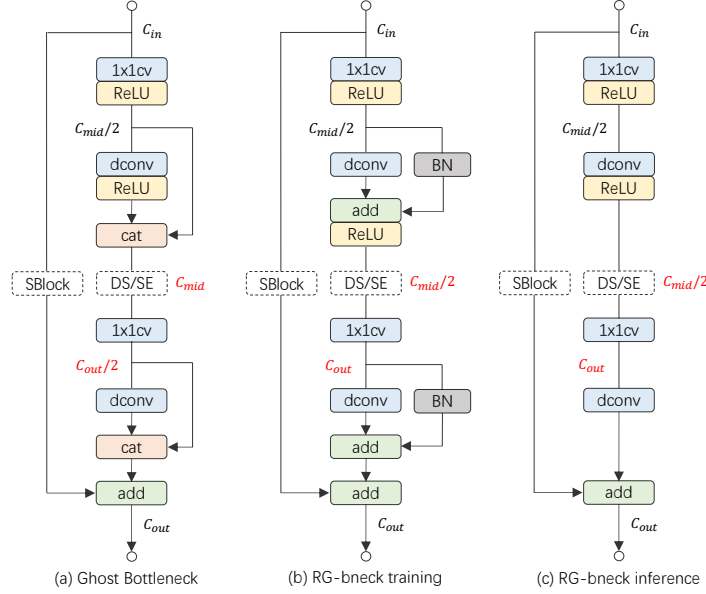
Figure 4: RepGhost bottleneck compared to Ghost bottleneck [13]. **1×1cv:** 1×1 convolutional layer, **SBlock:** shortcut block, **DS:** downsample layer, **SE:** SE block [20]. **RG-bneck:** RepGhost bottleneck. The blocks in dash line are only inserted if necessary. C_{in}, C_{mid} and C_{out} denote input, middle and output channels of the bottlenecks, respectively. Note that RepGhost bottleneck only differs to Ghost bottleneck in channels inside the bottlenecks, which are masked as red.

training same as Ghost module, but fuses them into C_{in} channels for fast inference, and thus lower FLOPs. That is, the difference between their output channels makes it non-trivial to improve Ghost module by directly using RepGhost module.

3.3 Building our Bottleneck and Architecture

RepGhost Bottleneck. Due to the change of output channels, this subsection introduces how to set channels properly to utilize RepGhost module to build our RepGhost bottleneck. As shown in Figure 4, our RepGhost bottleneck keeps the input and output channels of Ghost bottleneck [13] and replaces the two Ghost modules with our RepGhost modules directly. As Figure 4b shows, RepGhost bottleneck has two changes in channel setting: a) "thinner" middle channels, and b) "thicker" channels for second depthwise convolutional layer. Firstly, applying downsample and SE on feature maps with decreased channels makes RepGhost bottleneck more efficient [36]. Secondly, applying depthwise convolution on feature maps with increased channels enlarges the network capacity [38], thus making RepGhost bottleneck more effective. During inference, RepGhost bottleneck only contains 2 branches (4c): a shortcut and a single chain of operators (1×1, depthwise convolution and ReLU), making it more efficient in memory cost and fast inference [32, 10]. We also extent the bottleneck to MobileNetV4 [35] and verify its efficiency and effectiveness in Appendix B.1.

RepGhostNet. With the RepGhost bottleneck built above and its input and output channel numbers same as Ghost bottleneck, RepGhostNet can be simply built by replacing Ghost bottleneck in Ghost-Net [13] with our RepGhost bottleneck. The architecture detail is shown in Table 2. RepGhostNet stacks RepGhost bottlenecks except the input and output layers. A dense convolutional layer with 16 channels processes the input data, and a stack of normal 1×1 convolutions and average pooling predicts the final outputs. We slightly change the middle channels in group 4 to keep channels non-decreasing in this group [36]. We also apply SE block [20] and use ReLU as the non-linearity function in RepGhostNet as GhostNet [13] does. Following [32, 13], a *width multiplier* α is used to scale the network, which is denoted as RepGhostNet $\alpha\times$.

Table 2: Overall architecture of RepGhostNet. #mid means the middle channel, it correspondences to $C_{mid}/2$ in Figure 4. #out means the output channel. SE indicates whether to use SE blocks.

Input	Operator	#mid	#out	SE	Stride
$224^2 \times 3$	Conv3 × 3	-	16	-	2
$112^2 \times 16$	RG-bneck	8	16	-	1
$112^2 \times 16$	RG-bneck	24	24	-	2
$56^2 \times 24$	RG-bneck	36	24	-	1
$56^2 \times 24$	RG-bneck	36	40	1	2
$28^2 \times 40$	RG-bneck	60	40	1	1
$28^2 \times 40$	RG-bneck	120	80	-	2
$14^2 \times 80$	RG-bneck	100	80	-	1
$14^2 \times 80$	RG-bneck	120	80	-	1
$14^2 \times 80$	RG-bneck	120	80	-	1
$14^2 \times 80$	RG-bneck	240	112	1	1
$14^2 \times 112$	RG-bneck	336	112	1	1
$14^2 \times 112$	RG-bneck	336	160	1	2
$7^2 \times 160$	RG-bneck	480	160	-	1
$7^2 \times 160$	RG-bneck	480	160	1	1
$7^2 \times 160$	RG-bneck	480	160	-	1
$7^2 \times 160$	RG-bneck	480	160	1	1
$7^2 \times 160$	Conv1 × 1	-	960	-	1
$7^2 \times 960$	AvgPool	-	960	-	-
$1^2 \times 960$	Conv1 × 1	-	1280	-	1
$1^2 \times 1280$	Conv1 × 1	-	1000	-	1

3.4 Re-parameterization for Fast Inference

Our RepGhostNet is built with re-parameterization for implicit feature reuse, making its topology to be able to be further simplified for fast inference. However, re-parameterization is often used to improve performances and does not change their topology and latency [9, 45]. But we note that this performance gains on light-weight CNNs are marginal, as shown in Table 3, in which we apply re-parameterization to MobileNetV3 [18] and GhostNet [13] same as RepGhostNet. It is interesting that re-parameterization brings no performance gain to GhostNet, which is designed to reuse features explicitly via concatenation. While re-parameterization also reuses features, but implicitly, so it does not benefit GhostNet more.

Our RepGhostNet, however, is the first to reuse features implicitly via re-parameterization technique and produces a simplified topology for fast inference. As we will show in Table 4, compared to GhostNet 0.5×, 1.0× and 1.3×, our RepGhostNet 0.5×, 1.0× and 1.3× get not only 0.2∼0.5% higher accuracy but also significant speedup, *i.e.*, **16.5∼21.0%** faster on the mobile device.

Table 3: Effects of re-parameterization on two light-weight CNNs.

Model	Reparam	Top1 Acc.(%)
MobileNetV3 Small 1.0×	✗	67.7
	✓	68.0(+0.3)
GhostNet 0.5×	✗	66.4
	✓	66.4(+0.0)

4 Experiments

In this section, to show the superiority of the proposed RepGhostNet, we evaluate the architecture on ImageNet 2012 classification benchmark [8], MS COCO 2017 object detection and instance segmentation benchmarks [29] and make a fair comparison with other SOTA light-weight CNNs.

Table 4: Classification results on ImageNet. We compare RepGhostNet to SOTA light-weight CNNs.

Model	Params(M)	FLOPs(M)	Latency(ms)	Top-1 (%)	Top-5 (%)
ShuffleNetV2 0.5×[32]	1.4	41	-	61.1	82.6
MobileNetV2 0.5×[38]	2.0	97	41.9	65.6	86.3
MobileNeXt 0.35×[50]	1.8	80	34.1	67.7	-
MobileNetV3 Small 0.75×[18]	2.0	44	26.0	65.4	86.0
MobileNetV3 Small 1.0×[18]	2.5	57	31.9	67.7	87.5
GhostNet 0.5x[13]	2.6	42	31.7	66.4	86.6
RepGhostNet 0.5×	2.3	43	**25.1**	**66.9**	**86.9**
RepGhostNet 0.58×	2.5	60	**31.9**	**68.9**	**88.4**
ShuffleNetV2 1.0×[32]	2.6	146	-	69.4	88.9
MobileNetV2 0.75×[38]	2.2	141	78.2	70.6	89.6
MobileNetV3 Large 0.75×[18]	4.0	155	72.0	73.5	91.2
GhostNet 1.0×[13]	5.2	141	74.5	74.0	91.5
RepGhostNet 1.0×	4.1	142	**62.2**	**74.2**	**91.5**
RepGhostNet 1.11×	4.5	170	**71.5**	**75.1**	**92.2**
ShuffleNetV2 1.5×[32]	3.5	299	-	72.6	90.6
MobileNetV2 1.0×[38]	3.5	300	106.7	73.3	91.1
MobileNeXt 1.0×[50]	3.4	300	113.6	74.0	-
MobileOne-S0[45]	2.1	275	79.4	71.4	-
ProxylessNAS[27]	4.1	320	128.0	74.6	92.2
EfficientNet B0[42]	5.3	386	298.0	77.1	93.3
MobileNetV3 Large 1.0×[18]	5.4	219	95.2	75.2	92.4
GhostNet 1.3×[13]	7.3	226	117.6	76.2	92.9
RepGhostNet 1.3×	5.5	231	**92.9**	**76.4**	**92.9**
RepGhostNet 1.5×	6.6	301	**116.9**	**77.5**	**93.5**

Datasets. ImageNet has been a standard benchmark for visual models. It contains 1,000 classes with 1.28M training images and 50k validation images. We use all the training data and evaluate models on the validation images. Top-1 and Top-5 accuracy with single crop are reported.

MS COCO is also a well-known visual benchmark. We train our models using COCO 2017 $trainval35k$ split and evaluate on the $minival$ split with 5K images, following the open-source mmdetection [4] library.

Latency. Tensor compute engine MNN [25] is a light-weight framework for deep learning and provides efficient inference on mobile devices. So we use MNN to evaluate the latency of the models on the ARM-based mobile device using single thread. Batch size is set to 1 by default if not stated. Each model runs for 100 times and the latency is recorded as their average. Specifically, the used mobile device is **Xiaomi 5× with Qualcomm Snapdragon 625 processor**. More latency evaluations on other mobile devices will be provided in the Appendix A, including 3 more Android devices with different computational resources and an iPhone12.

4.1 ImageNet Classification

To demonstrate the effectiveness and efficiency of our proposed RepGhostNet, we compare to SOTA light-weight CNNs in terms of accuracy on ImageNet benchmark and latency on mobile devices.

Implementation Details. We adopt PyTorch [34] and timm [47] library for training. The global batch size is set to 1024 on 8 NVIDIA V100 GPUs. Standard SGD with momentum coefficient of 0.9 is the optimizer. Base learning rate is 0.6 and cosine anneals for 300 epochs with first 5 epochs for warming up, and weight decay is set as 1e-5. Dropout rate before classifier layer is set to 0.2. We also use EMA (Exponential Moving Average) weight averaging with 0.9999 factor. For data augmentation, except regular image crop and flip in timm, we also utilize random erase with prob 0.2. For larger models, $e.g.$, RepGhostNet 1.3× (231M), auto-augmentation [6] is applied. For fair comparison, we also retrain MobileNetV2, MobileNetV3 and GhostNet using our training settings.

Effective and Efficient. As Figure 1 and Table 4 show, RepGhostNet outperforms other SOTA light-weight CNNs in terms of accuracy-latency trade-off, including manually designed and NAS-based ones, $e.g.$, RepGhostNet 0.5× is **20%** faster than GhostNet 0.5× with 0.5% higher Top-1 accuracy, and RepGhostNet 1.0× is 14% faster than MobileNetV3 Large 0.75× with 0.7% higher

Table 5: Detection and instance segmentation results on COCO dataset.

Backbone	YOLOv3		RetinaNet		Mask RCNN	
	Latency(s)	mAP	Latency(s)	mAP	mAP^{bbox}	mAP^{mask}
MobileNetV2 1.0×	585.5	23.9	3.85	32.1	34.2	31.3
MobileNetV3 1.0×	580.3	23.8	3.70	32.7	34.2	31.5
GhostNet 1.1×	559.0	23.9	3.70	32.5	34.8	31.9
RepGhostNet 1.11×	**497.1**	**23.9**	**3.63**	**32.7**	**35.0**	**32.0**
RepGhostNet 1.3×	**555.3**	**24.7**	3.64	33.5	36.1	33.1

Top-1 accuracy. With comparable latency, RepGhostNet surpasses all models by a large margin in all FLOPs levels, *e.g.*, our RepGhostNet 0.58× surpasses GhostNet 0.5× by **2.5%** Top-1 accuracy.

4.2 Object Detection and Instance Segmentation

To verify the generalization of our RepGhostNet as a general backbone, we conduct experiments on COCO [29] object detection and instance segmentation benchmarks using mmdetection [4] library and compare with several other backbones in the tasks.

Implementation Details. We use YOLOv3 [37] and RetinaNet [28], and Mask RCNN [15] baselines for detection task and instance segmentation task, respectively. Following [4], we only replace the ImageNet-pretrained backbones and train the models for 12 epochs in 8 NVIDIA V100 GPUs. Synchronized BN is also enabled. We report the mAP@IoU of 0.5:0.05:0.95 and evaluate the latency of single-stage models, *i.e.*, YOLOv3 and RetinaNet.

Results. As the results shown in 5, our RepGhostNet outperforms MobileNetV2 [38], MobileNetV3 [18], and GhostNet [13] in both tasks in terms of accuracy-latency trade-off. For example, with comparable latency, RepGhostNet 1.3× surpasses all other backbones in both tasks clearly, and RepGhostNet 1.1× achieves comparable or even better performance with significant speedup.

4.3 Ablation Study

Comparison to MobileOne. We evaluate RepGhostNet on an iPhone12 to compare with MobileOne. As shown in Table 6, RepGhostNet 1.5× and 2.0× outperforms MobileOne in accuracy-latency trade-off, especially on iPhone12 CPU. Besides, we note that the reported latency in MobileOne paper [45] are evaluated on NPU, while we use CPU, which we conjecture causes the latency difference. More detailed comparisons are provided in Appendix A.4.

Table 6: Accuracy and latency on iPhone12.

Model	Top1 Acc.(%)	Latency(ms)	
		NPU	CPU
MobileOne-S2	77.4	1.20	12.18
RepGhostNet 1.5×	**77.5**	**1.15**	**9.15(+25%)**
MobileOne-S3	78.1	1.50	15.97
RepGhostNet 2.0×	**78.8**	**1.48**	**10.90(+32%)**

Re-parameterization Structures. To verify the re-parameterization structures of RepGhostNet, we alternate the components in the identity mapping branch (of module in Figure 3c) of RepGhostNet 0.5×, such as BN, 1×1 depthwise convolution and identity mapping itself [10, 45, 9]. Table 7 shows that re-parameterization with BN achieves the best performance, and we take it as our default structure for all other RepGhostNets. We attribute this improvement to the training-time non-linearity of BN, which provides more information than identity mapping. The 1×1 depthwise convolution is also

Table 7: Results of different re-parameterization structures on RepGhostNet 0.5×.

Variant	id	1×1dconv	BN	Top-1(%)
no-reparam				66.3
	✓			66.4
		✓		66.2
			✓	**66.9**
		✓	✓	66.5
	✓	✓	✓	66.5
+ReLU			✓	66.6

followed by BN, therefore, its parameters have no effort on the features due to the following normalization and may make the BN statistics unstable, which may result in its poor performance. Note that all the models in Table 7 can be fused into a same efficient inference model, expect the last one row. Specially, we insert a ReLU after 3×3 convolution like Ghost module to verify that it is safe to

move the ReLU backward, as we did in Figure 3*c*. Besides, compared to MobileOne [45], our re-parameterization structure is much simpler, *i.e.*, only one BN layer. The simpler re-parameterization structure makes negligible the additional training costs. For example, training RepGhostNet 0.5× with and without re-parameterization for 300 epochs cost 25.0 and 24.8 hours, respectively.

5 Conclusion

To utilize feature reuse in light-weight CNNs architecture design efficiently, this paper proposes a new perspective to realize feature reuse implicitly via structural re-parameterization technique, instead of the widely-used but inefficient concatenation operation. With this technique, a novel and hardware-efficient RepGhost module for implicit feature reuse is proposed. The proposed RepGhost module fuses features from different layers at training time, and carry out the fusion process in the weight space before inference, resulting in a simplified and hardware-efficient architecture for fast inference. Built on RepGhost module, we develop a hardware-efficient light-weight CNNs named RepGhostNet, which achieves new SOTA on several vision tasks in terms of accuracy-latency trade-off for mobile devices.

References

[1] Martín Abadi, Ashish Agarwal, Paul Barham, Eugene Brevdo, Zhifeng Chen, Craig Citro, Greg S Corrado, Andy Davis, Jeffrey Dean, Matthieu Devin, et al. Tensorflow: Large-scale machine learning on heterogeneous systems, 2015.

[2] Sajid Anwar, Kyuyeon Hwang, and Wonyong Sung. Structured pruning of deep convolutional neural networks. *ACM Journal on Emerging Technologies in Computing Systems (JETC)*, 13(3):1–18, 2017.

[3] Jin Chen, Xijun Wang, Zichao Guo, Xiangyu Zhang, and Jian Sun. Dynamic region-aware convolution. In *Proceedings of the IEEE/CVF Conference on Computer Vision and Pattern Recognition*, pages 8064–8073, 2021.

[4] Kai Chen, Jiaqi Wang, Jiangmiao Pang, Yuhang Cao, Yu Xiong, Xiaoxiao Li, Shuyang Sun, Wansen Feng, Ziwei Liu, Jiarui Xu, et al. Mmdetection: Open mmlab detection toolbox and benchmark. *arXiv preprint arXiv:1906.07155*, 2019.

[5] François Chollet. Xception: Deep learning with depthwise separable convolutions. In *Proceedings of the IEEE conference on computer vision and pattern recognition*, pages 1251–1258, 2017.

[6] Ekin D Cubuk, Barret Zoph, Dandelion Mane, Vijay Vasudevan, and Quoc V Le. Autoaugment: Learning augmentation policies from data. *arXiv preprint arXiv:1805.09501*, 2018.

[7] Mostafa Dehghani, Yi Tay, Anurag Arnab, Lucas Beyer, and Ashish Vaswani. The efficiency misnomer. In *International Conference on Learning Representations*, 2021.

[8] Jia Deng, Wei Dong, Richard Socher, Li-Jia Li, Kai Li, and Li Fei-Fei. Imagenet: A large-scale hierarchical image database. In *2009 IEEE conference on computer vision and pattern recognition*, pages 248–255. Ieee, 2009.

[9] Xiaohan Ding, Yuchen Guo, Guiguang Ding, and Jungong Han. Acnet: Strengthening the kernel skeletons for powerful cnn via asymmetric convolution blocks. In *Proceedings of the IEEE/CVF international conference on computer vision*, pages 1911–1920, 2019.

[10] Xiaohan Ding, Xiangyu Zhang, Ningning Ma, Jungong Han, Guiguang Ding, and Jian Sun. Repvgg: Making vgg-style convnets great again. In *Proceedings of the IEEE/CVF Conference on Computer Vision and Pattern Recognition*, pages 13733–13742, 2021.

[11] Shuxuan Guo, Jose M Alvarez, and Mathieu Salzmann. Expandnets: Linear over-parameterization to train compact convolutional networks. *Advances in Neural Information Processing Systems*, 33:1298–1310, 2020.

[12] Zichao Guo, Xiangyu Zhang, Haoyuan Mu, Wen Heng, Zechun Liu, Yichen Wei, and Jian Sun. Single path one-shot neural architecture search with uniform sampling. In *European conference on computer vision*, pages 544–560. Springer, 2020.

[13] Kai Han, Yunhe Wang, Qi Tian, Jianyuan Guo, Chunjing Xu, and Chang Xu. Ghostnet: More features from cheap operations. In *Proceedings of the IEEE/CVF conference on computer vision and pattern recognition*, pages 1580–1589, 2020.

[14] Kai Han, Yunhe Wang, Chang Xu, Jianyuan Guo, Chunjing Xu, Enhua Wu, and Qi Tian. Ghostnets on heterogeneous devices via cheap operations. *International Journal of Computer Vision*, 130(4):1050–1069, 2022.

[15] Kaiming He, Georgia Gkioxari, Piotr Dollár, and Ross Girshick. Mask r-cnn. In *Proceedings of the IEEE international conference on computer vision*, pages 2961–2969, 2017.

[16] Kaiming He, Xiangyu Zhang, Shaoqing Ren, and Jian Sun. Deep residual learning for image recognition. In *Proceedings of the IEEE conference on computer vision and pattern recognition*, pages 770–778, 2016.

[17] Yihui He, Xiangyu Zhang, and Jian Sun. Channel pruning for accelerating very deep neural networks. In *Proceedings of the IEEE international conference on computer vision*, pages 1389–1397, 2017.

[18] Andrew Howard, Mark Sandler, Grace Chu, Liang-Chieh Chen, Bo Chen, Mingxing Tan, Weijun Wang, Yukun Zhu, Ruoming Pang, Vijay Vasudevan, et al. Searching for mobilenetv3. In *Proceedings of the IEEE/CVF international conference on computer vision*, pages 1314–1324, 2019.

[19] Andrew G Howard, Menglong Zhu, Bo Chen, Dmitry Kalenichenko, Weijun Wang, Tobias Weyand, Marco Andreetto, and Hartwig Adam. Mobilenets: Efficient convolutional neural networks for mobile vision applications. *arXiv preprint arXiv:1704.04861*, 2017.

[20] Jie Hu, Li Shen, and Gang Sun. Squeeze-and-excitation networks. In *Proceedings of the IEEE conference on computer vision and pattern recognition*, pages 7132–7141, 2018.

[21] Yiming Hu, Yuding Liang, Zichao Guo, Ruosi Wan, Xiangyu Zhang, Yichen Wei, Qingyi Gu, and Jian Sun. Angle-based search space shrinking for neural architecture search. In *European Conference on Computer Vision*, pages 119–134. Springer, 2020.

[22] Gao Huang, Shichen Liu, Laurens Van der Maaten, and Kilian Q Weinberger. Condensenet: An efficient densenet using learned group convolutions. In *Proceedings of the IEEE conference on computer vision and pattern recognition*, pages 2752–2761, 2018.

[23] Gao Huang, Zhuang Liu, Laurens Van Der Maaten, and Kilian Q Weinberger. Densely connected convolutional networks. In *Proceedings of the IEEE conference on computer vision and pattern recognition*, pages 4700–4708, 2017.

[24] Sergey Ioffe and Christian Szegedy. Batch normalization: Accelerating deep network training by reducing internal covariate shift. In *International conference on machine learning*, pages 448–456. PMLR, 2015.

[25] Xiaotang Jiang, Huan Wang, Yiliu Chen, Ziqi Wu, Lichuan Wang, Bin Zou, Yafeng Yang, Zongyang Cui, Yu Cai, Tianhang Yu, Chengfei Lv, and Zhihua Wu. Mnn: A universal and efficient inference engine. In *MLSys*, 2020.

[26] Glenn Jocher. YOLOv5 by Ultralytics, 5 2020.

[27] Do-Guk Kim and Heung-Chang Lee. Proxyless neural architecture adaptation at once. *IEEE Access*, 10:99745–99753, 2022.

[28] Tsung-Yi Lin, Priya Goyal, Ross Girshick, Kaiming He, and Piotr Dollár. Focal loss for dense object detection. In *Proceedings of the IEEE international conference on computer vision*, pages 2980–2988, 2017.

[29] Tsung-Yi Lin, Michael Maire, Serge Belongie, James Hays, Pietro Perona, Deva Ramanan, Piotr Dollár, and C Lawrence Zitnick. Microsoft coco: Common objects in context. In *European conference on computer vision*, pages 740–755. Springer, 2014.

[30] Zechun Liu, Haoyuan Mu, Xiangyu Zhang, Zichao Guo, Xin Yang, Kwang-Ting Cheng, and Jian Sun. Metapruning: Meta learning for automatic neural network channel pruning. In *Proceedings of the IEEE/CVF international conference on computer vision*, pages 3296–3305, 2019.

[31] Zhenhua Liu, Zhiwei Hao, Kai Han, Yehui Tang, and Yunhe Wang. Ghostnetv3: Exploring the training strategies for compact models. *arXiv preprint arXiv:2404.11202*, 2024.

[32] Ningning Ma, Xiangyu Zhang, Hai-Tao Zheng, and Jian Sun. Shufflenet v2: Practical guidelines for efficient cnn architecture design. In *Proceedings of the European conference on computer vision (ECCV)*, pages 116–131, 2018.

[33] Pavlo Molchanov, Stephen Tyree, Tero Karras, Timo Aila, and Jan Kautz. Pruning convolutional neural networks for resource efficient inference. *arXiv preprint arXiv:1611.06440*, 2016.

[34] Adam Paszke, Sam Gross, Francisco Massa, Adam Lerer, James Bradbury, Gregory Chanan, Trevor Killeen, Zeming Lin, Natalia Gimelshein, Luca Antiga, et al. Pytorch: An imperative style, high-performance deep learning library. *Advances in neural information processing systems*, 32, 2019.

[35] Danfeng Qin, Chas Leichner, Manolis Delakis, Marco Fornoni, Shixin Luo, Fan Yang, Weijun Wang, Colby Banbury, Chengxi Ye, Berkin Akin, et al. Mobilenetv4-universal models for the mobile ecosystem. *arXiv preprint arXiv:2404.10518*, 2024.

[36] Ilija Radosavovic, Raj Prateek Kosaraju, Ross Girshick, Kaiming He, and Piotr Dollar. Designing network design spaces. In *Proceedings of the IEEE/CVF Conference on Computer Vision and Pattern Recognition (CVPR)*, June 2020.

[37] Joseph Redmon and Ali Farhadi. Yolov3: An incremental improvement. *arXiv preprint arXiv:1804.02767*, 2018.

[38] Mark Sandler, Andrew Howard, Menglong Zhu, Andrey Zhmoginov, and Liang-Chieh Chen. Mobilenetv2: Inverted residuals and linear bottlenecks. In *Proceedings of the IEEE conference on computer vision and pattern recognition*, pages 4510–4520, 2018.

[39] Rupesh Kumar Srivastava, Klaus Greff, and Jürgen Schmidhuber. Highway networks. *arXiv preprint arXiv:1505.00387*, 2015.

[40] Christian Szegedy, Wei Liu, Yangqing Jia, Pierre Sermanet, Scott Reed, Dragomir Anguelov, Dumitru Erhan, Vincent Vanhoucke, and Andrew Rabinovich. Going deeper with convolutions. In *Proceedings of the IEEE conference on computer vision and pattern recognition*, pages 1–9, 2015.

[41] Mingxing Tan, Bo Chen, Ruoming Pang, Vijay Vasudevan, Mark Sandler, Andrew Howard, and Quoc V Le. Mnasnet: Platform-aware neural architecture search for mobile. In *Proceedings of the IEEE/CVF Conference on Computer Vision and Pattern Recognition*, pages 2820–2828, 2019.

[42] Mingxing Tan and Quoc Le. Efficientnet: Rethinking model scaling for convolutional neural networks. In *International conference on machine learning*, pages 6105–6114. PMLR, 2019.

[43] Yehui Tang, Kai Han, Jianyuan Guo, Chang Xu, Chao Xu, and Yunhe Wang. Ghostnetv2: enhance cheap operation with long-range attention. *Advances in Neural Information Processing Systems*, 35:9969–9982, 2022.

[44] Han Vanholder. Efficient inference with tensorrt. In *GPU Technology Conference*, volume 1, page 2, 2016.

[45] Pavan Kumar Anasosalu Vasu, James Gabriel, Jeff Zhu, Oncel Tuzel, and Anurag Ranjan. Mobileone: An improved one millisecond mobile backbone. In *Proceedings of the IEEE/CVF Conference on Computer Vision and Pattern Recognition*, pages 7907–7917, 2023.

[46] Alvin Wan, Xiaoliang Dai, Peizhao Zhang, Zijian He, Yuandong Tian, Saining Xie, Bichen Wu, Matthew Yu, Tao Xu, Kan Chen, et al. Fbnetv2: Differentiable neural architecture search for spatial and channel dimensions. In *Proceedings of the IEEE/CVF Conference on Computer Vision and Pattern Recognition*, pages 12965–12974, 2020.

[47] Ross Wightman. Pytorch image models. `https://github.com/rwightman/pytorch-image-models`, 2019.

[48] Bichen Wu, Xiaoliang Dai, Peizhao Zhang, Yanghan Wang, Fei Sun, Yiming Wu, Yuandong Tian, Peter Vajda, Yangqing Jia, and Kurt Keutzer. Fbnet: Hardware-aware efficient convnet design via differentiable neural architecture search. In *Proceedings of the IEEE/CVF Conference on Computer Vision and Pattern Recognition*, pages 10734–10742, 2019.

[49] Xiangyu Zhang, Xinyu Zhou, Mengxiao Lin, and Jian Sun. Shufflenet: An extremely efficient convolutional neural network for mobile devices. In *Proceedings of the IEEE conference on computer vision and pattern recognition*, pages 6848–6856, 2018.

[50] Daquan Zhou, Qibin Hou, Yunpeng Chen, Jiashi Feng, and Shuicheng Yan. Rethinking bottleneck structure for efficient mobile network design. In *European Conference on Computer Vision*, pages 680–697. Springer, 2020.

Appendix

A   More Latency Evaluations

A.1   More mobile phones

We evaluate the latency of all models in main paper on Xiaomi 5× with **Qualcomm Snapdragon 625 processor**, which is considered as a low-end one nowadays. To verify the generalization of our RepGhost module and RepGhostNet to other mobile devices, we evaluate the latency on other three Android mobile phones with more powerful processors. They are Xiaomi Note3, Xiaomi 8 and Huawei P20 with **Qualcomm Snapdragon 660 processor**, **Qualcomm Snapdragon 845 processor** and **Kirin 970 processor**, respectively.

We plot the accuracy-latency results in Figure 5a, Figure 5b and Figure 5c same as Figure 1 in main paper. From these results, we can see similar trends of the curves, *i.e.*, our RepGhostNet outperforms other state-of-the-art light-weight CNNs in accuracy-latency trade-off in all four level mobile phones. Besides, note that the results vary widely between the four mobile phones, *e.g.*, the latency of RepGhostNet 1.0× on them vary from 22.3ms to 62.2ms, which means that our RepGhost module and RepGhostNet generalize well to wide range of mobile devices with different computational resources.
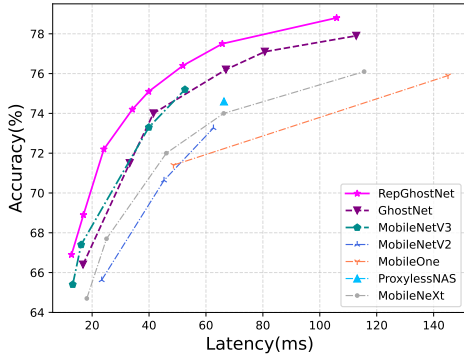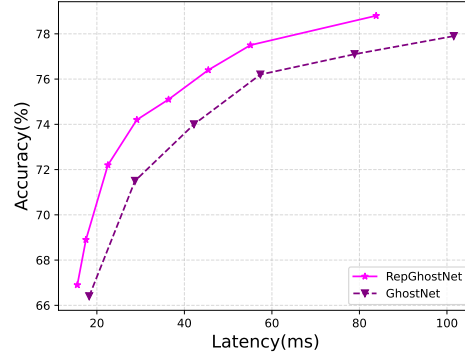

(a) Xiaomi Note3 with the **Snapdragon 660** processor.
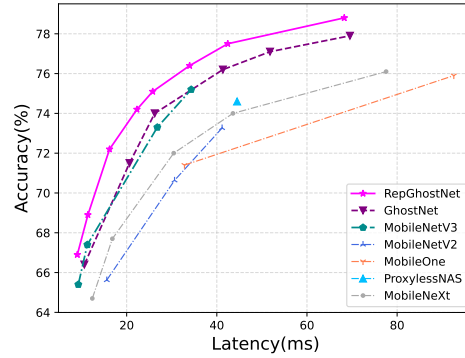
(b) Xiaomi 8 with the **Snapdragon 845** processor.
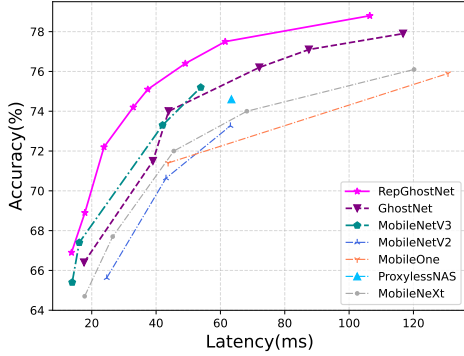
(c) Huawei P20 with the **Kirin 970** processor.

(d) **TFLite**.

Figure 5: Top-1 accuracy on ImageNet *vs.* latency of different devices (a,b,c) or compute engine (d).

A.2   Evaluation with TFLite

While we use MNN [25] as our mobile compute engine for all models, we also evaluate the models using TFLite[3] [1] in Figure 5d. We only compare RepGhostNet to GhostNet for convenience. As

---

[3]`https://github.com/tensorflow/tensorflow/tree/master/tensorflow/lite/tools/benchmark/android`

Figure 5d shows, we can observer similar trend of accuracy-latency as using MNN, verifying the generalization of our method. For example, compared to GhostNet 1.0× and 1.5×, RepGhostNet 1.0× and 1.5× gets not only 0.2% and 0.4% higher Top1 accuracy, but also **31.0% and 30.2% speedup**, respectively. Compared to MNN, TFLite brings more speedup of our RepGhostNet over GhostNet, thanks to the data layout of NHWC in TFLite, which makes the concatenation process in GhostNet more complicated, as we stated in Section 3.1 in main paper. Therefore, the elimination of the latency bottleneck at concatenation operation in our RepGhostNet brings much better latency performance.

A.3 Shortcut verification on these mobile phones

Removing shortcut is concerned in CNNs architecture design recently [10, 45]. To verify its necessity in light-weight CNNs, we remove the shortcut in RepGhostNet and evaluate its latency and accuracy on ImageNet. To be specific, we only remove the shortcuts of identity mapping and keep shortcut blocks for downsampling, so as to keep the model parameters and FLOPs for fair comparison. Statistically, there are 11 shortcuts of identity mapping removed in RepGhostNet. We train models with and without shortcut using the same training setting and re-parameterization structure.

We evaluate the latency performance of the networks with and without shortcuts in these mobile devices. As shown in Table 8, it is clear that shortcut does not affect the actual runtime severely, but help the optimization process [16]. On the other hand, removing shortcut of larger model (RepGhostNet 2×) brings less impact on accuracy compared to smaller models, which may means that shortcut is more important to light-weight CNNs than large models, *e.g.*, RepVGG [10] and MobileOne [45]. Considering all of this, we confirm that shortcut is necessary for light-weight CNNs and keep the shortcut in our RepGhostNet.

Table 8: Latency and accuracy results of RepGhostNet with and without shortcut on four mobile phones. 625, 660, 845 and 970 denote the corresponding processors.

RepGhostNet	Shortcut	Top1 Acc.(%)	Latency(ms)			
			625	660	845	970
0.5×	✓	66.9	25.1	13.0	9.0	13.7
	✗	64.1(-2.8)	24.9(-0.2)	12.8(-0.2)	8.8(-0.2)	13.7(-0.0)
1.0×	✓	74.2	62.2	34.2	22.3	32.9
	✗	72.7(-1.5)	60.5(-1.7)	33.5(-0.7)	22.1(-0.2)	31.6(-1.3)
1.5×	✓	77.5	116.9	65.7	42.4	61.5
	✗	75.8(-1.7)	114.9(-0.2)	64.8(-0.9)	41.9(-0.5)	61.4(-0.1)
2.0×	✓	78.8	190.0	105.9	68.3	106.4
	✗	77.9(-0.9)	186.7(-3.3)	104.3(-1.6)	67.5(-0.8)	103.8(-2.6)
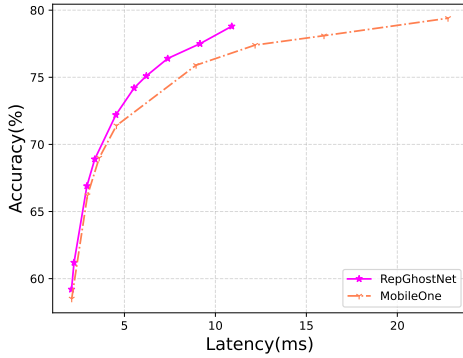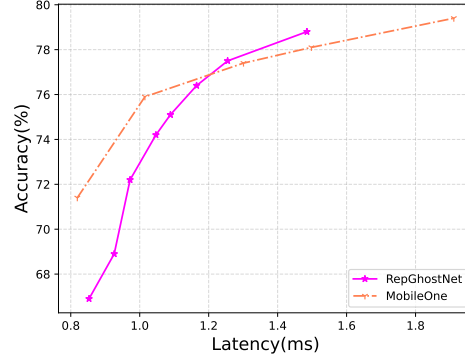
(a) **iPhone12 CPU**   (b) **iPhone12 NPU**

Figure 6: Top-1 accuracy on ImageNet *vs.* latency on iPhone12.

A.4 Comparison to MobileOne on iPhone

MobileOne [45] is also a recent mobile CNN, but designed for iPhone. We provide the detailed accuracy-latency comparison of our RepGhostNet to MobileOne[4] [45] on the CPU and NPU[5] of an iPhone12 in Figure 6a and Figure 6b, respectively. While our RepGhostNet is designed for mobile CPU, it also outperforms MobileOne on iPhone12 CPU clearly as shown in Figure 6a, same as other Android mobile phones we evaluated above. As for iPhone12 NPU in Figure 6b, for extremely low FLOPs CNNs, RepGhostNet does not perform as well as MobileOne and RepGhostNet $1.5\times$ and $2.0\times$ outperform it. We conjecture that it is caused by the difference between CPU and NPU. With a strong parallel computing capability, NPU prefers to models with larger FLOPs than those with lower FLOPs, motivating us to design larger and more efficient CNNs for powerful NPUs in the future.

B Generalization of RepGhost

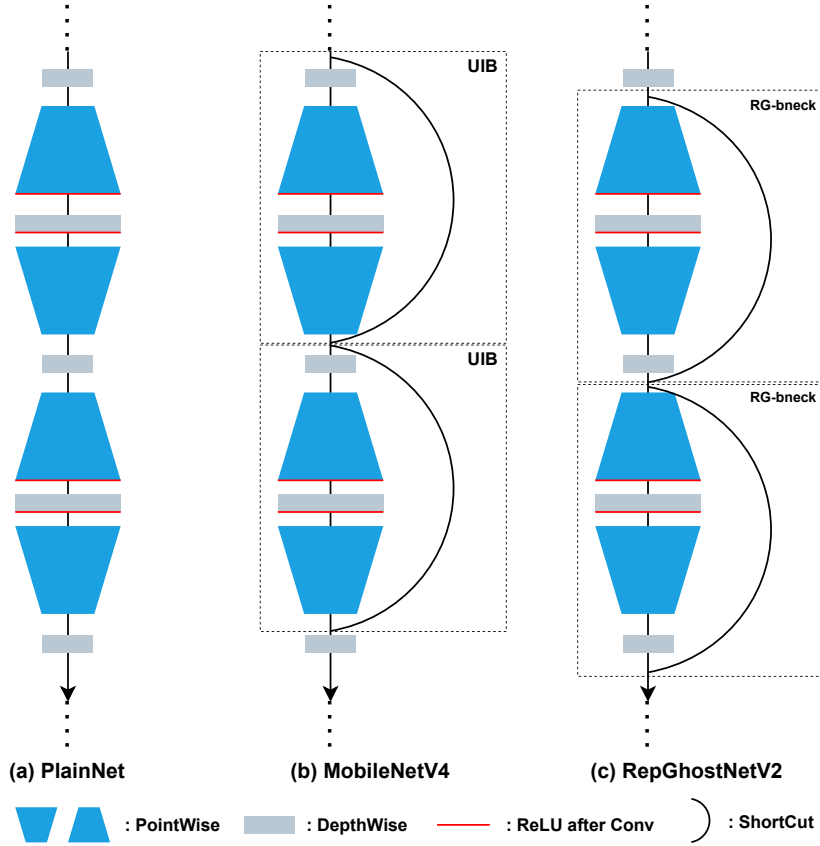### B.1 Generalization to MobileNetV4

Figure 7: Architecture comparison of MobileNetV4 and our RepGhostNetV2. (a) The plain net without shortcuts. (b) MobileNetV4. (c) Our RepGhostNetV2 has the same architecture as MobileNetV4, but only differs in the shortcut connections.

With the re-parameterization technique, we derive our novel RepGhost bottleneck in Figure 4c, whose efficiency and effectiveness are proven in the main paper. In the subsection, we use this bottleneck to evolve MobileNetV4 to our another novel network RepGhostNetV2, and also verify its architecture design again.

---

[4]`https://github.com/apple/ml-mobileone/tree/main/ModelBench`
[5]It is known as Apple Neural Engine (ANE) in iPhone, which is also a kind of Neural Processing Unit (NPU).

MobileNetV4 [35] is a newly efficient light-weight CNNs for diverse mobile devices; it introduces a novel Universal Inverted Bottleneck (UIB) to build the efficient networks. Same as RepGhost bottleneck in Figure 4c, UIB consists of two depthwise and two pointwise convolutional layers, but differs in the layer orders, *i.e.*, '3-1-3-1' in UIB and '1-3-1-3' in ours, where 3 and 1 denote the kernel sizes and further depthwise and pointwise convolutional layers, respectively.

In this glance, when all shortcuts are removed from an UIB or RepGhost bottleneck based network, they both produce a MobileNetV1-like networks [19], *i.e.*, alternating order of depthwise and pointwise convolutional layers like '...3-1-3-1-3-1...' layer chain without shortcuts, as PlainNet shown in Figure 7a. With this layer chain, we simply change the way of shortcut connection from UIB to our RepGhost bottleneck, thus producing our novel network in Figure 7c, which is denoted as *RepGhostNetV2*.

With the same architectures except the way of shortcut connections, our RepGhostNetV2 has **exactly the same parameters and FLOPs** compared to MobileNetV4. To evaluate their performance, we simply utilize the training setting introduced in Section 4 to both networks. Note that re-parameterization technique is not applied to RepGhostNetV2 during training. We also evaluate their latency on iPhone12 NPU. As shown in Table 9, RepGhostNetV2 gets similar latency on iPhone12 and comparable performance to MobileNetV4, indicating the efficiency and effectiveness of our RepGhost bottleneck. That is, as alternatives to UIB and MobileNetV4, our RepGhost bottleneck RepGhostNetV2 can also served as an efficient building block and light-weight CNNs for diverse mobile devices.

It is also interesting that the plain net underperforms to these two networks, but with similar latency. This proves again that the shortcuts do not affect latency but help the optimizations a lot, same as our verification in Appendix A.3.

Table 9: Results of MobileNetV4 and RepGhostNetV2.

Model Size	Image Size	Epoch	Model	Top1 Acc(%)	iPhone12 Latency(ms)
Small	224	300	PlainNet	70.7	0.99
			MobileNetV4	72.3	1.01
			RepGhostNetV2	72.3	1.01
Medium	256	300	PlainNet	71.6	1.47
			MobileNetV4	79.5	1.48
			RepGhostNetV2	79.5	1.48
Large	384	300	PlainNet	76.8	3.58
			MobileNetV4	81.5	3.63
			RepGhostNetV2	81.5	3.63

B.2 Generalization to YOLOv5

To verify the replacing of concatenation to add operators, we replace the concatenation operators in $C3$ modules of YOLOv5 [26] with add ones and keep the output channels of $C3$ modules the same. The result in Table 10 shows the superior of our method.

Table 10: Results of YOLOv5. The models are in float16 and evaluated on a V100 GPU. Batch size are set to 32 and 1 for throughput and latency evaluations, respectively.

Model	Ops	mAP	Throughput	Latency(ms)
YOLOv5n	Concatenation	27.5	2078	1.31
	Add	**27.6**	**2169(+4.4%)**	**1.21(+7.3%)**
YOLOv5s	Concatenation	36.1	1635	1.65
	Add	**36.1**	**1757(+7.5%)**	**1.51(+8.5%)**

B.3 Comparison to GhostNetV2 and GhostNetV3

GhostNetV2 [43] augments GhostNet with DFC attention, which can be applied to improve RepGhost-Net directly. Specifically, as a long-range attention, DFC is inserted after the first Ghost module of each Ghost bottleneck. Following this, we can build our RepGhostNet with DFC attention simply by inserting it after the first RepGhost module. Note that our first RepGhost module has only half the number of channels compared to that of the first Ghost module, making the attention lighter. We evaluate the latency using TFLite same as Section A.2. We also retrain GhostNetV2 using our setting and achieve accuracy similar to their reported results [43]. As Table 11 shows, when equipped with DFC attention, RepGhostNet gets comparable performance to GhostNetV2 with less parameters and lower FLOPs, and even significant speedup, $e.g.$, more than **34.0% faster**.

With the same architecture to GhostNetV2, GhostNetV3 [31] utilizes advanced training techniques, including dedicated training hyper parameters and distillation strategy, to greatly improve the performance. As shown in Figure 8, our network obtains similar Pareto Frontiers to GhostNetV3 in terms of accuracy-latency trade-off, not to mention we only apply simple but effective training settings.

Table 11: Comparison of RepGhostNet + DFC and GhostNetV2 [43].

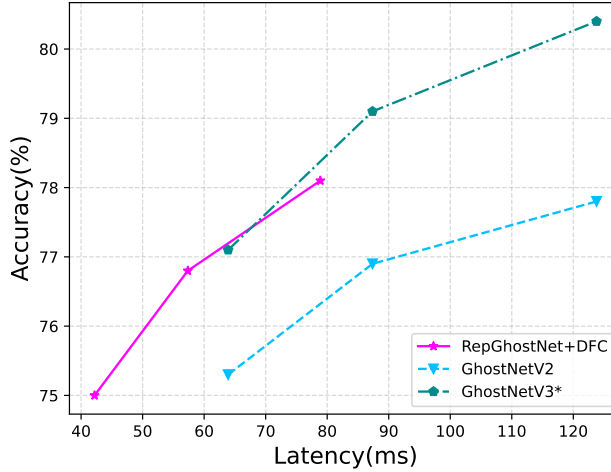| Model	α	Top1 Acc(%)	Params(M)	FLOPs(M)	Latency(ms)
	1.0	**75.3**	6.1	167	63.9
GhostNetV2	1.3	**76.9**	8.9	269	87.4
	1.6	77.8	12.3	399	123.8
RepGhostNet	1.0	75.0	**4.6**	**156**	**42.2(+34.0%)**
+	1.3	76.8	**6.3**	**254**	**57.4(+34.3%)**
DFC	1.6	**78.1**	**8.4**	**370**	**78.9(+36.3%)**

Figure 8: Accuracy **vs.** latency of RepGhostNet + DFC, GhostNetV2 and GhostNetV3. We retrain GhostNetV2 using our training setting. *We directly use the reported results of GhostNetV3 here, which utilizes advanced training techniques.

B.4 Comparison to Ghost-R50

To verify the generation of RepGhost module to large models, $i.e.$, ResNet50 [16], we compare it to Ghost-R50 as reported in [13]. We replace the Ghost module in Ghost-R50 with our RepGhost module to get RepGhost-R50. All models are trained with the same training setting. MNN latency is evaluated the same as other models on the mobile device. For TRT latency, we first convert the models to TensorRT [44], then run each model on the framework for 100 times on a T4 GPU with batch size 32, and report the average latency. The results is shown in Table 12. We can see that RepGhost-R50 is faster than Ghost-R50 significantly in both CPU and GPU with comparable accuracy. Specially,

Table 12: Results on comparison with Ghost-R50 [13].

Model	Params(M)	FLOPs(B)	MNN Latency(ms)	TRT Latency(ms)	Top-1(%)
Ghost-R50 (s=2)	14.0	2.2	610.6	64.8	76.2
RepGhost-R50 (s=1.4)	13.2	2.2	**547.1(+10.4%)**	**56.5(+12.8%)**	**76.2**
Ghost-R50 (s=4)	8.2	1.2	423.9	70.2	73.1
RepGhost-R50 (s=2)	7.1	1.2	**331.6(+21.8%)**	**38.9(+44.6%)**	**73.6**

RepGhost-R50 (s=2) gets **21.8% and 44.6% speedup** over Ghost-R50 (s=4) in MNN and TensorRT inferences, respectively.

C Impact Statements

This paper proposes a light-weight CNN architecture whose goal is to improve the efficiency of CNNs for mobile devices, $i.e.$, less computational resources and higher accuracy. With this positive impact, we believe our model will make deep learning on computer vision much more widely and easily accessible, especially for people from less developed areas.

As a data-driven deep learning architecture, our RepGhostNet compares to other state-of-the-art light-weight CNNs using public datasets in our work, like ImageNet and COCO, which verify its efficiency and effectiveness. However, training our models using other datasets may lead to some dataset-related impacts which is beyond our scope and also faced by all other deep learning architectures. We leave it for future works.